



CHORUS

This is the accepted manuscript made available via CHORUS. The article has been published as:

Indications of an Electronic Phase Transition in Two-Dimensional Superconducting $\text{YBa}_{2}\text{Cu}_{3}\text{O}_{7-x}$ Thin Films Induced by Electrostatic Doping

Xiang Leng, Javier Garcia-Barriocanal, Boyi Yang, Yeonbae Lee, J. Kinney, and A. M. Goldman

Phys. Rev. Lett. **108**, 067004 — Published 10 February 2012

DOI: [10.1103/PhysRevLett.108.067004](https://doi.org/10.1103/PhysRevLett.108.067004)

Indications of an Electronic Phase Transition in $\text{YBa}_2\text{Cu}_3\text{O}_{7-x}$ Thin Films Induced by Electrostatic Doping

Xiang Leng, Javier Garcia-Barriocanal, Boyi Yang,

Yeonbae Lee, J. Kinney, and A. M. Goldman

School of Physics and Astronomy, University of Minnesota,

Minneapolis, Minnesota 55455, USA

Abstract

We successfully tuned an underdoped ultrathin $\text{YBa}_2\text{Cu}_3\text{O}_{7-x}$ film into the overdoped regime by means of electrostatic doping using an ionic liquid as a dielectric material. This process proved to be reversible. Transport measurements showed a series of anomalous features compared to chemically doped bulk samples and a different two-step doping mechanism for electrostatic doping was revealed. The normal resistance increased with carrier concentration on the overdoped side and the high temperature (180 K) Hall number peaked at a doping level of $p \sim 0.15$. These anomalous behaviors suggest that there is an electronic phase transition in the Fermi surface around the optimal doping level.

PACS numbers: 74.25.Dw, 74.25.F-, 74.40.Kb, 74.62.-c

Keywords:

The modulation of the electrical charge carrier density in strongly correlated electron systems using an electric field as an external control parameter is a long-standing goal in condensed matter physics due to its potential impact from both fundamental and technological points of view[1, 2]. Among those interesting materials, the application of field effect concepts to high temperature superconductors (HTSCs) is an active research field since it could provide a tool to control the density of the superconducting condensate in a reversible way, while keeping a fixed structure and avoiding changing the disorder associated with conventional doping by chemical substitution[3, 4]. Apart from potential applications, electrostatic doping of HTSCs is also a useful tool to study fundamental questions that still remain open such as the properties of the superconductor-insulator (SI) transition and the role of quantum criticality [5, 6].

Recently, the development of electronic double layer transistors (EDLT), that use ionic liquids (ILs) as gate dielectrics, has been successfully employed to achieve levels of doping of $10^{15}/\text{cm}^2$ [7–9]. Taking advantage of such large charge transfers, this technique has been employed to successfully tune the SI transition in $\text{La}_{2-x}\text{Sr}_x\text{CuO}_4$ (LSCO)[5] and in $\text{YBa}_2\text{Cu}_3\text{O}_{7-x}$ (YBCO)[6], and to study the low carrier concentration side of the phase diagram. Both works reveal interesting physics on the nature of the quantum phase transition separating the superconducting and insulating phases when the density of charge carriers is depleted.

Nonetheless, the possibility of accumulating charge carriers by the field effect to tune an underdoped cuprate into the overdoped regime has remained elusive. For the 123 family of cuprate compounds, it has been shown that the CuO_2 planes are only indirectly affected by the electric field since the injected holes are mainly induced in the CuO_x chains[10]. Moreover, the systematic preparation of YBCO bulk samples by tuning the oxygen stoichiometry in the overdoped region is difficult to achieve and the highest level of overdoping is limited by the oxygen stoichiometric concentration, 0.194 holes/Cu for $\text{YBa}_2\text{Cu}_3\text{O}_7$ [11].

Here we present a transport study of an electrostatically doped YBCO ultrathin film. We exploit the high local electric fields (10^9 V/m) induced by an ionic liquid at the surface of the sample to tune the concentration of holes in the superconducting condensate across the top of the superconducting dome. The experiment reveals that the electrostatic doping of YBCO involves a different doping mechanism, as well as an anomalous normal resistance behavior in the overdoped regime. Surprisingly, we also find that the Hall number measured

at 180 K displays a maximum around the optimal doping level that suggests the occurrence of an electronic phase transition separating the underdoped and overdoped regimes.

Ultrathin YBCO films were grown by means of a high pressure oxygen sputtering technique on (001) oriented SrTiO₃ substrates. The technical details of sample preparation and characterization can be found in Ref. [6]. In order to determine the thickness threshold that separates insulating and superconducting samples, i.e. the thickness of the dead layer, we produced a series of thin films with thicknesses ranging from 5 to 10 unit cells. Using standard four-probe techniques we characterized the $R(T)$ curves for each sample and we found that the 5-6 unit cell thick samples are insulating and the superconducting properties are completely recovered in a 7 unit cell thick film. The EDLT devices were fabricated using films of this thickness, following the procedure described in Ref. [8].

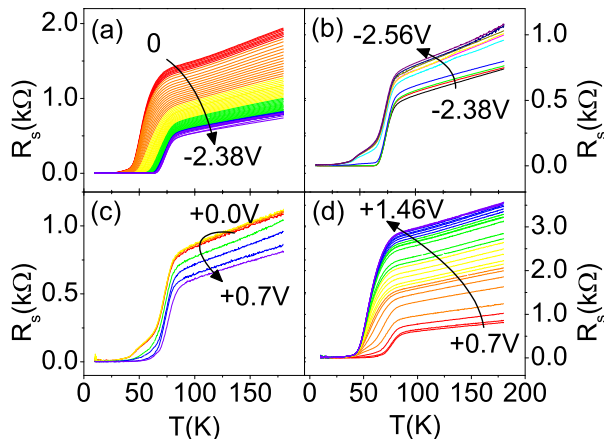


FIG. 1: (color online) Temperature dependence of the sheet resistance at different gate voltages. (a). From 0 to -1.2 V, V_G was changed in -0.1 V increments and then from -1.2 to -2.38 V, the increment was -0.02 V. (b). From -2.38 to -2.56 V, V_G was changed in increments of -0.02 V. (c). Negative V_G was then removed and a positive V_G was added. From 0 to 0.7 V, V_G was changed in 0.1 V increments. (d). $V_G = 0.7, 0.75, 0.80, 0.85, 0.90, 0.95, 1.0, 1.05, 1.07, 1.10, 1.13, 1.15, 1.17, 1.20$ V, then the increment was changed to 0.02 V until $V_G = 1.46$ V.

We monitored the gating process of the 7 unit cell YBCO ultrathin film by measuring the sheet resistance as a function of temperature (see Fig. 1). The fresh sample, without any applied gate voltage (V_G), has a transition temperature $T_c = 42$ K. We determined T_c as the temperature corresponding to the crossing of the extrapolation of the fastest falling part of the $R(T)$ curve to zero resistance. After the application of a negative gate voltage,

T_c increases and the normal state sheet resistance (the metallic region of the curve) drops. For higher negative gating, $V_G = -2.24$ to -2.38 V, the rate of change of T_c and the normal resistance slows down and saturates. T_c reaches a maximum value of 67 K and the normal resistance reaches a minimum of 750Ω at 180 K. We also observed small fluctuations in both T_c and the normal resistance in this regime. As shown in Fig. 1(b), upon a further increase of the negative gate voltage, T_c decreases. In addition, the normal resistance increases with increasing negative gate voltage. For the highest negative gate voltages (-2.46 V $< V_G < -2.56$ V) we note that the superconducting transition is not abrupt and a second transition is turned on at the lowest temperature part of the $R(T)$ curve. Next we reversed the polarity of the gating (see Fig. 1(c)), and we observed that after a threshold voltage of about $+0.3$ V, T_c starts to increase and the normal resistance starts to drop. With further increase in the positive gate voltage, as shown in Fig. 1(d), T_c drops and the normal resistance increases, and the sample recovers its initial state.

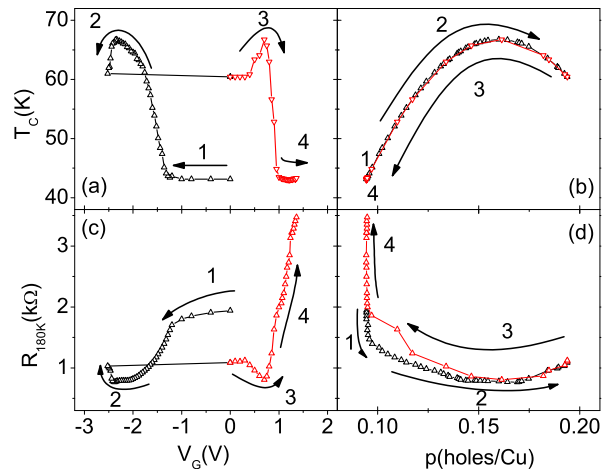


FIG. 2: (Color online) Top panel: Transition temperature vs. gate voltage (a) and effective hole doping (b). Bottom panel: Sheet resistance at 180 K vs. gate voltage (c) and effective hole doping (d). The sequence of the gating process is denoted by steps 1 to 4.

In order to analyze the dependence of the $R(T)$ curves as a function of gate voltage, we have plotted T_c and the normal resistance measured at 180 K versus V_G in Fig. 2(a) and Fig. 2(c). As can be expected, the application of a negative voltage accumulates holes in the thin film and both T_c and the normal state resistance change, increasing and decreasing respectively. This is an indication that charge carriers are being injected into the sample

and the concentration of holes is increasing towards the optimal doping point of the superconducting dome of high T_c cuprates. The subsequent drop of T_c suggests that the sample has been tuned into the overdoped regime, although the increase of the resistance in this regime is different from what is found in chemically doped bulk samples[12] and will be analyzed in detail later. By changing the polarity of V_G we check the reversibility of the process and rule out a possible chemical reaction on the sample's surface. The results confirm that the electrostatic doping process is reversible. Moreover, the measurements reveal that the dependence of the transport properties of the sample as function of gate voltage is hysteretic. The electronic double layer created at the interface between the ionic liquid and the cuprate is of the order of one nanometer in thickness and a Coulomb type interaction emerges between the surface anions from the ionic liquid and accumulated carriers (holes) in the film. To change the sign of the ions that covered the surface of the sample, and hence destroy the electronic double layer, a threshold gate voltage of reverse polarity is needed which could lead to the observed hysteretic dependence. In addition, anions and cations from the ionic liquid are different in size and molecular weight and an asymmetric response to positive or negative gate voltages can be expected.

In order to obtain an independent variable to describe the process of accumulation or depletion of holes we inferred an effective hole doping “ p ” by using the universal empiric parabolic relation $T_c/T_{c,\max} = 1 - 82.6(p - 0.16)^2$ [13], which has been proved to be true for bulk high T_c superconductors including 123 compounds[14]. Using this calculated number of holes we plot T_c and the values of normal resistance at 180 K in Fig. 2(b) and Fig. 2(d). The black open triangles represent the evolution of T_c and the normal resistance at 180 K during the accumulation of holes while the depletion process is represented by the red open triangles in both graphs. The estimated number of holes allows us to represent the superconducting dome of the sample removing the effects of the hysteretic dependence in gate voltage. We observed a maximum T_c of 67 K and we would like to point out that this value depends strongly on the criteria selected to calculate it. The superconducting transitions of ultrathin films are broad and the maximum T_c of the sample can be as high as 83 K if T_c is calculated from the onset transition temperature where the resistance drops to its 90 % value. Furthermore, all the samples of the present study are strained due to the thin film thicknesses, which are always bellow 12 nm, and a depressed superconducting transition temperature is expected due to the strong thickness dependence of T_c [15–17].

Upon a closer comparison of Fig. 2(b) and 2(d), we notice that the gate process steps 1 and 4 are different from steps 2 and 3. In steps 1 and 4, T_c remains constant but the normal resistance changes. While in steps 2 and 3, T_c and the normal resistance are correlated and change together. It is well known that in 123 compounds, the normal resistance is determined by the carriers both on the CuO_2 planes and on the CuO_x chains while T_c is mainly determined by the carriers on the CuO_2 planes[18]. Step 1 occurs at the beginning of the charging process and T_c remains the same suggesting that a threshold V_G is required for the carriers to be doped onto the CuO_2 planes. During step 1 only the normal state resistance changes, which would be an indication that the carriers can be induced only on the CuO_x chains. A similar behavior can be observed in step 4 once the sample has returned to its initial state. Here T_c remains constant suggesting that another threshold V_G is required to deplete the CuO_x chains and then start the depletion of carriers on the CuO_2 planes. In between there are steps 2 and 3 where the carriers on the CuO_2 planes can be induced reversibly by the electrostatic charging and thus the T_c and the normal resistance change together.

This data suggests that the electrostatic doping of YBCO is actually a two-step process. First carriers are induced only on the CuO_x chains, and second, once a threshold concentration is reached, carriers can be induced on the CuO_2 planes. In the second step, the carriers could be indirectly doped on the CuO_2 planes through intra-cell charge transfer[10]. This two-step electrostatic doping process appears to be different from that of chemical doping, in which any changes of the hole doping under the superconducting dome will affect the normal resistance and the superconducting properties simultaneously.

In Fig. 2(d) the normal resistance at 180 K exhibits a minimum at the optimal doping point. As stated before this is a surprising behavior since in the overdoped region of the general bulk phase diagram of cuprates, the normal state is a Fermi liquid and a lowering of the normal resistance would be expected as the doping level increases. To clarify this point we consider the screening length of the electric field for a non-perfect metal, which is given by the expression: $\lambda \propto \sqrt{\varepsilon/g(E_F)}$, where ε is the dielectric constant of the cuprate and $g(E_F)$ is the density of states at the Fermi energy [19]. By applying higher negative voltages to the gate electrode the number of holes increases and λ becomes shorter. Therefore, the screening of the electric field in a shorter length scale reduces the thickness of the active layer of the sample and would increase the sheet resistance accordingly. This suggest that the shortening

of the penetration depth, i.e. the reduction of the dimensionality of the sample, could have some contribution on the explanation of the increasing values of the sheet resistance and would explain the broader transition observed for the highest negative voltages. Indeed, for the shortest penetration depth of the electric field we would be observing a purely two dimensional superconductor, where the fluctuations of the Cooper pairs would produce the observed broadening of the superconducting transition that would be governed by a two dimensional Kosterlitz-Thoules mechanism. Nonetheless, we can estimate the dependence of the sheet resistance with λ using a 3D free electron model and assuming that the conductivity has a Drude behavior $\sigma = ne\mu$ and $g(E_F) \propto n^{1/3}$ (n is the 3D electron density and μ is the mobility). The sheet resistance would take the form $R_s = 1/(\sigma\lambda) \propto 1/(n^{5/6}\mu)$ and based on this estimation, the increase of the carrier density will always cause the sheet resistance to drop contrary to what we observed. One possibility to explain our results is that the surface scattering might increase during the gating process and cause the mobility to drop as more carriers accumulate at the surface. This should be a general property of the gating process, but previous experiments using ionic liquids as gate dielectrics showed that the mobility usually increases and then saturates as V_G increases[7, 20], or behaves similar to those chemically bulk doped samples[21, 22], or gradually decreases ($\sim 10\%$ in total) with an increasing V_G [23]. We believe that this would rule out the effect of the mobility in explaining the increasing values of resistance at the overdoped side. It could suggest that it is caused by a significant change of $g(E_F)$ together with the shortening of the screening length of the electric field.

To get further insight into this behavior we measured the Hall resistance at 180 K at different gate voltages. Figure 3 shows the normalized Hall number (n_H) as a function of V_G (a) and effective doping (b). The Hall number is calculated using $n_H = 1/(R_{He})$, R_H being the Hall coefficient determined from the slope of the linear fit of the Hall resistance vs. magnetic field. Interestingly, we find that the Hall number shows a peak at a doping level of $p \sim 0.15$ holes/Cu ($V_G = -2.24$ V) which does not coincide with the maximum and minimum of T_c and the normal resistance respectively ($p = 0.16$ holes/Cu or $V_G = -2.38$ V). Moreover, in between these levels of doping we observe fluctuations in both T_c and the normal resistance.

The Hall effect of high- T_c cuprates has been extensively studied and two scenarios have been proposed. One is the two relaxation time model[24, 25], in which the Hall relaxation

rate $1/\tau_H$ and the transport scattering rate $1/\tau_{tr}$ are associated with spins and charges respectively. In the other scenario the scattering arising from different regions of the Fermi surface is considered[26]. Experimentally, an anomalous dependence of the normal state Hall coefficient on the doping level has been reported in chemically doped YBCO[27], $\text{Bi}_2\text{Sr}_{1.51}\text{La}_{0.49}\text{CuO}_{6+\delta}$ (BSLCO) [28] and LSCO[29]. For YBCO the Hall conductivity at 125 K showed an anomalous behavior around the 60-K phase and in BSLCO and LSCO, the Hall number peaks around the optimal doping level at low temperature when superconductivity is suppressed by an ultra high magnetic field. These anomalous behaviors are commonly interpreted with an unusual electronic state or a sudden change in the Fermi surface, although chemical doping might also change the magnetic coupling and thus the Hall scattering rate. For electrostatic doping, we don't believe that an electric field would change the magnetic coupling. The n_H peak then suggests that an electronic phase transition is occurring, which is supported by the emergence of fluctuations in T_c and the normal state resistance at this same level of doping.

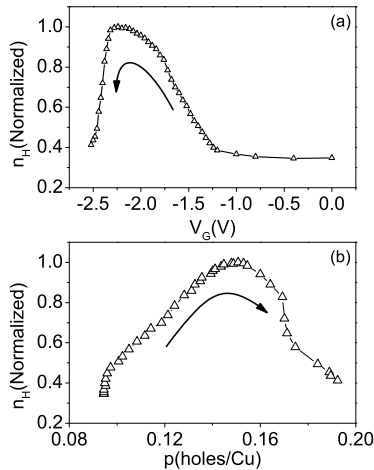


FIG. 3: Normalized Hall number (n_H) vs. gate voltage (a) and effective hole doping (b).

Moreover, in our results, the peak of the Hall number is found to be at $p \sim 0.15$, to the left of the optimal doping point ($p = 0.16$). For a doping level of $p \sim 0.15$ the value expected for T^* , the pseudogap crossover temperature, roughly matches 180 K [30]. Quantum oscillation experiments[18, 31–33] showed that while there is a large hole-like Fermi surface in the overdoped regime, there are only small pockets in the underdoped regime. Angle Resolved Photoemission Spectroscopy also showed that the transition from the overdoped to the underdoped regime is accompanied by an electronic reconstruction of the Fermi surface[34–38].

Thus an electronic phase transition which would reconstruct the Fermi surface is expected around the optimal doping regime and could be confirmed by our measurements.

In summary, we have studied the transport properties of an ultrathin YBCO film with the doping level changing from the underdoped regime to the overdoped regime by means of electrostatic doping. Our results reveal a two-step doping mechanism for the electrostatic doping of YBCO which is different from that of conventional chemical doping. Anomalous behavior of the normal resistance on the overdoped side was also accompanied by a peak in the high temperature (180 K) Hall number at $p \sim 0.15$. This suggests there is an electronic phase transition on the Fermi surface near the optimal doping point. The low dimensionality of the film or the high local electric field in the EDLT configuration might enhance this electronic phase transition and bring about these anomalous behaviors.

We would like to thank S. Bose for his assistance with sample preparation, C. Geppert for his help with measurements and B. Skinner for useful discussions. This work was supported by the National Science Foundation under grants NSF/DMR-0709584 and 0854752. Part of this work was carried out at the University of Minnesota Characterization Facility, a member of the NSF-funded Materials Research Facilities Network via the MRSEC program, and the Nanofabrication Center which receives partial support from the NSF through the NNIN program. JGB thanks the Spanish Ministry of Education for the financial support through the National Program of Mobility of Human Resources (2008-2011).

-
- [1] C. H. Ahn et al., *Rev. Mod. Phys.* **78**, 1185 (2006).
 - [2] C. H. Ahn et al., *Science* **284**, 1152 (1999).
 - [3] M. Imada, A. Fujimori, and Y. Tokura, *Rev. Mod. Phys.* **70**, 1039 (1998).
 - [4] J. Mannhart, *Supercond. Sci. Technol.* **9**, 49 (1996).
 - [5] A. T. Bollinger et al., *Nature* **472**, 458 (2011).
 - [6] X. Leng et al., *Phys. Rev. Lett.* **107**, 027001 (2011).
 - [7] J. T. Ye et al., *Nat Mater* **9**, 125 (2010).
 - [8] Y. Lee et al., *Phys. Rev. Lett.* **106**, 136809 (2011).
 - [9] H. Shimotani et al., *Applied Physics Letters* **91**, 082106 (2007).
 - [10] M. Salluzzo et al., *Phys. Rev. Lett.* **100**, 056810 (2008).

- [11] R. Liang, D. A. Bonn, and W. N. Hardy, Phys. Rev. B **73**, 180505 (2006).
- [12] S. H. Naqib et al., Physica C **387**, 365 (2003).
- [13] M. R. Presland et al., Physica C **176**, 95 (1991).
- [14] J. L. Tallon et al., Phys. Rev. B **51**, 12911 (1995).
- [15] L. X. Cao et al., Phys. Rev. B **65**, 113402 (2002).
- [16] M. Salluzzo et al., Phys. Rev. B **72**, 134521 (2005).
- [17] M. Varela et al., Phys. Rev. Lett. **83**, 3936 (1999).
- [18] N. Doiron-Leyraud et al., Nature **447**, 565 (2007).
- [19] B. Skinner et al., Phys. Rev. E **83**, 056102 (2011).
- [20] R. Scherwitzl et al., Advanced Materials **22**, 5517 (2010).
- [21] K. Ueno et al., Nat Mater **7**, 855 (2008).
- [22] K. Ueno et al., Nat Nano **6**, 408 (2011).
- [23] H. Yuan et al., Advanced Functional Materials **19**, 1046 (2009).
- [24] P. W. Anderson, Phys. Rev. Lett. **67**, 2092 (1991).
- [25] T. R. Chien, Z. Z. Wang, and N. P. Ong, Phys. Rev. Lett. **67**, 2088 (1991).
- [26] B. P. Stojković and D. Pines, Phys. Rev. Lett. **76**, 811 (1996).
- [27] K. Segawa and Y. Ando, Phys. Rev. Lett. **86**, 4907 (2001).
- [28] F. F. Balakirev et al., Nature **424**, 912 (2003).
- [29] F. F. Balakirev et al., Phys. Rev. Lett. **102**, 017004 (2009).
- [30] J. L. Tallon et al., physica status solidi (b) **215**, 531 (1999).
- [31] C. Jaudet et al., Phys. Rev. Lett. **100**, 187005 (2008).
- [32] B. Vignolle et al., Nature **455**, 952 (2008).
- [33] D. LeBoeuf et al., Nature **450**, 533 (2007).
- [34] M. R. Norman et al., Nature **392**, 157 (1998).
- [35] K. M. Shen et al., Science **307**, 901 (2005).
- [36] M. Platé et al., Phys. Rev. Lett. **95**, 077001 (2005).
- [37] M. A. Hossain et al., Nat Phys **4**, 527 (2008).
- [38] M. R. Norman, Physics **3**, 86 (2010).